Articles in PresS. Am J Physiol Regul Integr Comp Physiol (January 6, 2010). doi:10.1152/ajpregu.00650.2009

The cellular force-frequency response in ventricular myocytes from the varanid lizard, *Varanus exanthematicus*

Daniel E. Warren[1*], Gina L.J. Galli[2], Simon M. Patrick[1] and Holly A. Shiels[1]

Faculty of Life Sciences

[1]University of Manchester, Core Technology Facility, Manchester, UK, M13 9NT

[2]Land and Food Systems, University of British Columbia, Vancouver, BC, Canada V6T 1Z4

Running head: Frequency and contractile function in varanid cardiomyocytes

*Contact Information:

Daniel E. Warren

University of California, San Francisco

Department of Anesthesia and Perioperative Care, Box 0542

San Francisco, CA, 94143

E-mail: warrend@anesthesia.ucsf.edu

Phone: 415.476.6231

Fax: 415.476.8841

Abstract

To investigate the cellular mechanisms underlying the negative force-frequency relationship (FFR) in the ventricle of the varanid lizard, *Varanus exanthematicus*, we measured sarcomere and cell shortening, intracellular Ca^{2+} ($[Ca^{2+}]_i$), action potentials (APs) and K^+ currents in isolated ventricular myocytes. Experiments were conducted between 0.2-1.0 Hz, which spans the physiological range of *in vivo* heart rates at 20-22°C for this species. As stimulation frequency increased, diastolic length, percent change in sarcomere length and relaxation time all decreased significantly. Shortening velocity was unaffected. These changes corresponded to a faster rate of rise of $[Ca^{2+}]_i$, a decrease in $[Ca^{2+}]_i$ transient amplitude, and a seven-fold increase in diastolic $[Ca^{2+}]_i$. The time constant for the decay of the Ca^{2+}transient (τ) decreased at higher frequencies, indicating a frequency dependent acceleration of relaxation (FDAR), but then reached a plateau at moderate frequencies and did not change above 0.5 Hz. The rate of rise of the AP was unaffected, but the AP duration (APD) decreased with increasing frequency. Peak depolarization tended to decrease, but was only significant at 1.0 Hz. The decrease in APD was not due to frequency-dependent changes in the delayed inward rectifier (I_{Kr}) or the transient outward (I_{to}) current as neither appeared to be present in varanid ventricular myocytes. Our results suggest that a negative FFR relationship in varanid lizard ventricle is caused by decreased amplitude of the Ca^{2+} transient coupled with an increase in diastolic Ca^{2+}, which leads to incomplete relaxation between beats at high frequencies. This coincides with shortened action potential duration (APD) at higher frequencies.

Keywords: action potential, calcium, diastolic Ca^{2+}, IK_1, IK_r, Ito, reptile, sarcomere shortening

Introduction

Heart rate is an important determinant of cardiac output and chronotropic changes have long been known to influence the force generated during a cardiac contraction (7, 53). The change in force production and contractility with increasing heart rate, or contraction frequency, is termed the force-frequency relationship (FFR) (14, 43), and can be classified as positive, primary-phase negative, secondary-phase negative, or overall negative (14). In mammals, the shape of the FFR varies with species, temperature, and even between cell populations within the same ventricle (17). Rodents tend to be more variable in this regard while larger mammals generally show a positive FFR. Among ectotherms, most fishes show a negative FFR (40, 41, 43) while frogs and reptiles (including turtles, lizards, and snakes) tend to show a secondary phase negative response that is flat or positive at low frequencies and negative at high frequencies (12, 18, 37). With the exception of fishes (26), the cellular mechanisms underlying FFR in other ectothermic animals, including reptiles, have not been studied.

Changes in force development are directly related to changes in the intracellular Ca^{2+} transient (54). The Ca^{2+} transient is the transient rise and fall of cytosolic Ca^{2+} that links excitation of the myocyte membrane to contraction of the myofilaments through a process known as excitation-contraction (E-C) coupling (2-4). Calcium enters the myocyte through voltage-gated L-type Ca^{2+} channels ($I_{Ca\text{-}L}$) and triggers further Ca^{2+} release from the sarcoplasmic reticulum (SR) ryanodine receptors (RyR) that then activates the contractile machinery. Relaxation occurs when Ca^{2+} is either pumped back into the SR via SR Ca^{2+}-ATPases (SERCA) or across the sarcolemma via the Na^{+}/Ca^{2+} exchanger (NCX). The contribution of each component to E-C coupling depends on factors that include metabolic state (30), species (1), temperature (39), ontogeny (23) and tissue type (atrial or ventricular)(50). E-C

coupling mechanisms in vertebrate ectotherms are variable in regards to the relative importance of the SR as a source of activator Ca^{2+}. Turtles and amphibians show little or no SR involvement (6, 20, 46), while SR Ca^{2+} contribution is variable in fishes (28, 41) and lizards (6, 18, 21). Recent work on single myocytes from *Varanus exanthematicus*, a lizard with a comparatively large aerobic scope and enhanced cardiovascular function (24) compared to other reptiles, has shown that the SR contributes approximately 35% of the Ca^{2+} to the Ca^{2+} transient with the NCX and the $I_{Ca\text{-}L}$ making up the remainder (21). It has also been previously shown in muscle strip preparations that the varanid lizard ventricle shows a negative FFR (18).

In the present study, we investigated the FFR in isolated ventricular myocytes from the varanid lizard, *Varanus exanthematicus* with the following aims: 1) to characterize the FFR using sarcomere and cell shortening as indices for contractility, 2) to measure changes in intracellular Ca^{2+} in response to changes in frequency, and 3) to determine if changes in the action potential (AP) and associated K^+ channel currents contribute to the FFR.

Our results suggest that a negative FFR relationship in varanid lizard ventricle is caused by decreased amplitude of the Ca^{2+} transient coupled with an increase in diastolic Ca^{2+} which leads to incomplete relaxation between beats at high frequencies. This coincides with shortened action potential duration (APD) at higher frequencies. We discuss these results in the context of cardiac function and the FFR in vertebrates, generally, and reptiles and lizards, in particular.

Materials and Methods

Animal Origin and Care

Savannah monitor lizards, *Varanus exanthematicus,* (Mean ± SEM body mass = 67.26 ± 3.34 g and heart mass = 294.4 ± 16.9 mg, n = 9) were obtained from Monkfield Nutrition

(Hertfordshire, UK) and held in a large terrarium with basking lamps and access to a temperature gradient from 20-35ºC for behavioral thermoregulation with a 12:12 photoperiod. They were fed daily and had free access to water and shelter. The animal housing and procedures were in accordance with regulations of the UK Home Office.

Solutions

The solution used for isolating lizard ventricular myocytes was the same as described previously for turtles (20) and contained the following (in mM): 100 NaCl, 10 KCl, 1.2 KH_2PO_4, 4 $MgSO_4$, 50 taurine, 20 glucose, and 10 HEPES. The pH was adjusted to 6.9 with KOH. For enzyme digestion, this solution also contained 1.5 mg/ml collagenase (Type 1A), 0.5 g/ml trypsin (type IX) and 1.5 mg/ml fatty acid-free bovine serum albumin (BSA).

Unless otherwise noted, the composition of the extracellular solution was the same for all experiments and contained the following (in mM): 150 NaCl, 5.4 KCl, 1.5 $MgSO_4$, 0.4 NaH_2PO_4, 2 $CaCl_2$, 10 glucose and 10 HEPES. The pH was adjusted to 7.7 with NaOH. This solution is identical to similar studies of turtles (20) and a previous electrophysiological study of varanid cardiomyocytes (21). All drugs were obtained from Sigma except where indicated. Pipette solutions for AP measurements contained (in mM): 140 KCl, 5 MgATP, 0.025 EGTA, 1 $MgCl_2$ and 10 HEPES. The pH was adjusted to 7.2 with KOH. The pipette solution used in K^+ current recordings was identical to that in the AP recordings except that it contained 5 mM EGTA. While recording K^+ currents, the extracellular solution always contained tetrodotoxin (TTX, 0.5 μM), CdCl (200 μM), and glibenclamide (10 μM) to inhibit Na^+, Ca^{2+}, and ATP-sensitive K^+ channels, respectively (27).

Ventricular Myocyte Isolation

The method for isolating ventricular myocytes from varanid lizards was similar to that previously described for turtles and lizards (20, 21). The lizards were decapitated, their hearts removed, weighed, cannulated through the right aortic arch, and retrogradely perfused with enzyme/BSA-free isolation solution at 30ºC with a flow rate of 0.5-1 ml min^{-1}. This temperature was found to maximize the yield of viable cells from each preparation and was within the range of temperatures the lizards experience while housed at the University. After 10 min, the heart was perfused with the enzyme/BSA solution (see above) for an additional 20 min. The heart was then removed, and the ventricle was cut away from the atria and placed in fresh isolation solution. Ventricular tissue was then carefully cut in half mid-sagitally with scissors and gently shaken to liberate the dissociated myocytes. The cells were transferred to a clean centrifuge tube containing fresh isolation solution and were stored at room temperature and used within 8-10 hours.

Measurements of Sarcomere and Cell Shortening

Sarcomere length was recorded from field-stimulated myocytes perfused with extracellular solution on an inverted microscope (Nikon Diaphot) with an attached CCD camera (WAT-902B, Watec, Japan). The video was digitized (MU510, IonOptix, Milton, MA, USA) and processed with Ionwizard 6.0 software (IonOptix) where the average sarcomere length within the user-determined window was measured by averaging the periodicity of the Z-line density based on the fast Fourier transform algorithm. The kinetics of shortening were further analyzed using Clampfit 9.2 software (Molecular Devices) and included sarcomere shortening velocity, diastolic length, percent change in sarcomere length, and time to 50% relaxation. Each

cell was stimulated to contract twelve times at each frequency. The middle six contractions were averaged for analysis. Cells were only selected if they possessed clearly defined sarcomeres with a resting length above 1.8 μm and contracted in unison with the stimulation pulse.

Measurements were made at stimulation frequencies of 0.2, 0.3, 0.5, 0.8, and 1 and again at 0.2 Hz. The mean length of cells measured in this study was 165 ± 10 μm (mean ± SEM, *n*=8 cells from 4 animals). The effects of stimulation frequency on cell shortening was also quantified as the difference between systolic and diastolic cell length measured from one end of the myocyte (26).

Measurements of Intracellular Ca^{2+}

The effects of stimulation frequency on $[Ca^{2+}]_i$ were measured using Fura-2 dual-excitation, single-emission ratiometric imaging in field-stimulated isolated ventricular myocytes (*n*=7 cells from 3 animals). After pre-incubation in 5 μM Fura-2 AM for 15 min at room temperature, isolated ventricular myocytes were transferred to a perfusion bath mounted on an inverted microscope (Nikon Eclipse) and perfused for 2-3 minutes in extracellular solution (see above). The cells were alternately excited at 340 and 380 nm with a xenon arc-lamp and monochromator and 510 nm emission was detected with a photomultiplier (Optoscan Fluorescence System, Cairn Research Ltd, Kent, UK). Amplifier outputs were digitized (Axon Instruments Digitdata 1440; Sunnyvale, USA) and analyzed with software (Axon Instruments PCLAMP 10). Recordings were made in cells stimulated at 0.2, 0.3, 0.5, 0.8, 1.0, and 0.2 Hz.

The Fura dye was calibrated as previously described for trout cardiomyocytes (42). Briefly, Fura-loaded cells were perfused with extracellular solution containing 2 μM rotenone, 5 μM carbonyl cyanide *m*-chlorophenyl-hydrazone (CCCP), 5 mM sodium iodoacetate, and the

Ca^{2+} ionophore 4-bromo A23187. For determination of the fluorescence intensity ratio at maximal Ca^{2+} binding (Rmax), the solution also contained a total of 2 mM $CaCl_2$. For determination of the ratio at zero Ca^{2+} binding (Rmin), the solution was nominally Ca^{2+}-free and contained 10 mM EGTA. All ratiometric data were converted to $[Ca^{2+}]_i$ using K_d = 336 nM (31) and the equation of Grynkiewicz et al (25).

Measurements of APs and K^+ currents

The effects of stimulation frequency on APs and K^+ currents were measured with whole-cell current and voltage clamp-techniques, respectively. An Axopatch 200B amplifier equipped with a CV 203BU head-stage was coupled through a Digidata 1200 to a PC running pCLAMP 9 (Axon Instruments, Sunnyvale, CA). Myocytes were superfused in a recording chamber (RC-24, Warner Instruments) with EC solution at a rate of 1-2 ml min^{-1} at room temperature (~21^{o}C). Borosiliciate pipettes had a resistance of 2.50 ± 0.06 MΩ when filled with pipette solution. After rupturing the patch, the cell capacitive currents were compensated. Mean series resistance and capacitance were 10.3 ± 1.2 MΩ and 41.9 ± 3.2 pF, respectively (n = 17 cells from 4 animals).

Action potentials were recorded in current clamp mode and were elicited by 2 ms depolarizing pulses at 0.3, 0.5, 0.8, 1.0 and 0.3 Hz. Potassium channel recordings were obtained by adapting protocols previously used by Vornanen and colleagues in rainbow trout cardiomyocytes (27, 49). The presence of the delayed inward rectifier channel current (I_{Kr}) and the transient outward K^+ (I_{to}) were investigated with a series of seven pre-pulses between -80 and +60 mV in 20 mV steps as described previously (19). For measurement of background inward rectifier K^+ current (I_{K1}), one second repolarizing voltage ramps from +30 mV to -120 mV were applied at 5 sec intervals in the presence and absence of 500μM $BaCl_2$. The final I_{K1}

was calculated as the difference between the two treatments. Signals were analyzed offline using Clampfit 9.0 software (Axon Instruments).

Statistical Analysis

One-factor repeated measures ANOVA was used to determine if stimulation frequency affected any of the measured variables. When the data were not normally distributed, repeated measures ANOVA on Ranks was used. Student-Newman Keuls post-hoc tests were used to elucidate differences when they were detected. Data were considered significant when $P<0.05$. Statistical computations were carried out using SigmaStat 3.5 (Systat Software, Chicago, USA).

Results

Effects of stimulation frequency on sarcomere and cell shortening

To assess the effects of stimulation frequency on the contractility of isolated myocytes, we measured sarcomere (Fig. 1) and cell shortening (Table 1) when cells were stimulated at frequencies between 0.2 and 1.0 Hz. Increasing stimulation frequency had no statistical effect ($P>0.05$) on sarcomere shortening rate (Fig. 1B). Diastolic sarcomere length decreased nearly linearly and was significantly reduced at 0.3 Hz (Fig. 1C). Sarcomere shortening, expressed as a percentage change from diastolic length, was significantly decreased ($P<0.05$) only at the two highest frequencies, indicating a secondary-phase negative FFR (Fig. 1D). The time to 50% recovery of sarcomere length decreased with frequency and was significant ($P<0.05$) at 0.5 Hz, after which the rate continued to decline significantly (Fig. 1E). This change is, in part, attributed to the decrease in diastolic sarcomere length. All sarcomere shortening variables were

completely reversible upon return to 0.2 Hz except diastolic sarcomere length, which remained at a length equal to that observed at 0.3 Hz.

Cell shortening velocity (Table 1) was also unaffected ($P>0.05$) by frequency while cell shortening as a percent change decreased linearly ($P<0.05$) with increased frequency, indicating a negative FFR at this level of the myocyte. The recovery of cell length was similar to sarcomere length and was significantly decreased ($P<0.05$) at 0.5 Hz and continued to fall thereafter.

Effect of frequency on intracellular Ca^{2+}

To investigate the $[Ca^{2+}]_i$ changes that underlie the negative FFR observed in the shortening studies, $[Ca^{2+}]_i$ was assessed in Fura-2 loaded cells field-stimulated at 0.2-1.0 Hz. As frequency increased, the rise slope of $[Ca^{2+}]_i$ (Fig. 2B) and the transient amplitude (Fig. 2D) significantly decreased ($P<0.05$), indicating Ca^{2+} entry, either across the sarcolemma or from the SR, was reduced. Meanwhile, diastolic $[Ca^{2+}]_i$ (Fig. 2C) significantly increased ($P<0.05$) with frequency until 0.8 Hz. In the face of these changes, Tau (τ), the time constant of decay of the Ca^{2+} transient, decreased significantly ($P<0.05$) with increased frequency until 0.5 Hz, after which it remained constant (Fig. 2E). This indicates an initial enhancement of Ca^{2+} extrusion that reaches an upper limit of the cell's ability to extrude intracellular Ca^{2+} under the conditions of our study. The decrease in τ with increased frequency also shows that varanid lizard ventricular myocytes exhibit the phenomenon known as frequency dependent acceleration of relaxation (FDAR). The effects of frequency on all measured variables related to Ca^{2+} showed varying degrees of reversibility upon return to 0.2 Hz, with diastolic $[Ca^{2+}]_i$ and τ being completely reversible while rise slope and Ca^{2+} transient amplitude returned to levels observed at

0.5 Hz. This shows that the change in $[Ca^{2+}]_i$ were frequency-dependent and not caused by run-down of cells.

Effects of frequency on action potential and K^+ channels

To determine whether changes in the AP underlie the negative FFR observed, ventricular AP's from 0.3 to 1.0 Hz were recorded using the whole-cell current clamp technique (Fig. 3). As frequency increased, APD measured at 50% and 90% repolarization (Fig. 3E) significantly decreased ($P<0.05$). Peak depolarization tended to decrease with increasing frequency ($P>0.05$), but was only significant at 1.0 Hz ($P<0.05$). Stimulation frequency did not affect resting membrane potential (Vm) or the rate of rise of the AP ($P>0.05$; Fig. 3B and 3C).

To investigate some of the currents responsible for decreased APD with increasing frequency, we sought to measure the effect of frequency on I_{Kr} and I_{to} densities. However, protocols previously used to isolate I_{Kr} and I_{to} in tuna (19) failed to evoke a tail current (indicative of I_{Kr}) or an initial peak after the depolarizing test pulse (indicative of I_{to}) leading us to conclude that neither are present in varanid cardiac myocytes (data not shown)
In addition to the time-dependent K^+ currents, we investigated the background inward rectifier I_{K1} and verified its presence as an important repolarizing current in varanid ventricular myocytes (Fig. 4). However, I_{K1} will not contribute to frequency-dependant changes in APD because it is a time-independent current. In aggregate, these results suggest other ion currents are involved in the frequency-dependent change in APD in varanid hearts.

Discussion

The aims of this study were to characterize the FFR in unloaded isolated ventricular myocytes from varanid lizards at physiological frequencies and to determine how changes in intracellular Ca^{2+} and the AP might account for our observations. Sarcomere and cell shortening were confirmed as good indices of contractility as the negative relationship observed in the present study correlates with the negative FFR previously seen in stimulated ventricular strips from this species under similar conditions (18). In addition to this finding, our study showed the following: 1) the negative FFR correlates with a frequency-dependent decrease in the Ca^{2+} transient amplitude and rise slope and an increase in diastolic $[Ca^{2+}]_{i,}$ 2) the decay constant of the Ca^{2+} transient decreases and the rate of sarcomeric relaxation increases with increased frequency, and 3) although APD is reduced with increasing frequency, it is not due to changes in I_{Kr} or I_{to}. Our data suggest that the negative FFR and decreased $[Ca^{2+}]_i$ amplitude may be related to a limitation in the Ca^{2+} extrusion mechanisms, i.e. SERCA and the sarcolemmal NCX that leads to diastolic Ca^{2+} accumulation. All parameters measured in a frequency-dependent manner showed total or nearly complete reversibility, indicating run-down was not responsible for the pattern of changes observed.

Comparisons with other ectotherms

This is the first investigation into the cellular FFR in reptilian cardiac myocytes and only the second of vertebrate ectotherms, the other being in trout (26). Like varanid lizards, the trout ventricle shows a negative FFR in both muscle strips and isolated myocytes (12, 13, 26).

Isolated trout ventricular myocytes also show many qualitative similarities to varanid lizard myocytes in response to increased frequency, including decreases in resting length, Ca^{2+} transient amplitude, and APD and an increase in diastolic $[Ca^{2+}]_i$ (26).

One important difference between the varanid lizard and trout is that the former shows frequency-dependent acceleration of relaxation (FDAR), an important regulated phenomenon of mammalian cardiomyocytes (11) required to attain high heart rates. In mammals, FDAR results from a phospholamban-independent enhancement of SERCA function (11, 29, 33, 47) that decreases τ and relaxation time. The presence of FDAR in varanid lizard ventricular myocytes is not surprising given that this species is capable of high heart rates (compared with other ectotherms) and utilizes SR Ca^{2+} to a greater extent than the rainbow trout (21). The FDAR described in the present study provides a mechanistic explanation for the varanid lizard's ability to attain maximal heart rates that are higher than other vertebrate ectotherms (24, 52).

AP changes with frequency

Our inability to detect I_{Kr} or I_{to} suggests they are not present in varanid ventricular myocytes, indicating other ion currents probably account for the shortened APD at high frequencies. The absence of a I_{Kr} tail current in varanid lizard ventricular myocytes is consistent with the same finding in turtle ventricular myocytes (45), suggesting its absence is a general feature of reptiles. It is not, however, a feature of all lower vertebrates as I_{Kr} has been well-characterized in the hearts of bluefin tuna (19) and rainbow trout (27, 49) in which the same methodology was used. To our knowledge, I_{to} has not been documented in any ectothermic species and is somewhat variable in mammals, evoking a long or short APD phenotype

depending on species and anatomical region of the heart (35, 38). In some species, such as the guinea pig, I_{to} is absent entirely (48).

Other currents that are likely to be involved in APD regulation are the L-type Ca^{2+} channel current ($I_{Ca\text{-}L}$) and the slow delayed rectifier K^+ channel current (I_{Ks}) (9, 36). Indeed, reduced $I_{Ca\text{-}L}$ with increased frequency has been associated with shorter APD in ventricular myocytes from failing human hearts (32) and from trout (26), both of which show negative FFR. I_{Ks} is an important modulator of APD in mammalian cardiac myocytes (36), but this current has not been identified or characterized in ectothermic myocytes.

Vornanen et al (49) suggest the complete inhibition of I_{Kr} by low concentrations of E-4031 (a specific I_{Kr} inhibitor) and inward rectification due to rapid inactivation indicate that the delayed rectifier current of trout atrial and ventricular myocytes is almost exclusively carried by I_{Kr} and not I_{Ks}. However, since I_{Kr} appears absent in reptilian cardiac myocytes, I_{Ks} may play a more significant role in the varanid AP and frequency modulation. Further research into the underlying ion channels responsible for the AP configuration in varanid lizards will answer these questions more thoroughly.

The causes and consequences of elevated diastolic $[Ca^{2+}]_i$

The six-fold reversible increase in diastolic $[Ca^{2+}]_i$ was a striking finding in this study and so we discuss its potential causes in more detail. Cardiomyocytes can be considered to be in a dynamic steady-state where diastolic $[Ca^{2+}]_i$ is maintained by a balance between Ca^{2+} entry via $I_{Ca\text{-}L}$, reverse-mode NCX and RyR, and Ca^{2+} removal via forward-mode NCX and SERCA (3). In varanid lizard myocytes, diastolic $[Ca^{2+}]_i$ increases with increased frequency and although the Ca^{2+} transient amplitude decreases, the frequencies are high enough such that the total Ca^{2+} entry

rate (Ca^{2+} transient amplitude x frequency) increases. Despite the initial increase in Ca^{2+} removal rate (decreased τ), diastolic $[Ca^{2+}]_i$ still increases. This suggests that Ca^{2+} removal mechanisms are operating maximally at stimulation frequencies greater than 0.5 Hz under the conditions of our study. This raises the question: What limits the removal mechanisms at high frequencies in the varanid myocyte? Further research is required to address this question, but we discuss some key possibilities briefly below.

The first factor limiting Ca^{2+} efflux could be intracellular Na^+ accumulation. As frequency increases, Na^+ entry through voltage-gated Na^+ channels increases and can accumulate in the cytosol, thereby reducing Ca^{2+} extrusion via forward-mode NCX. Intracellular Na^+ activity (aNa^+) increases with stimulation frequency in trout (5) but not in rat, even though both show increases in diastolic Ca^{2+} (17). Canine heart also increased aNa^+ at high frequencies (8). It is possible that the slight but significant hyperpolarization in myocytes returning to 0.3 Hz from 1.0 Hz in the present study is due to Na/K ATPase stimulation caused by a transient Na^+ accumulation (51). There are no other data available to evaluate this mechanism, but given the similarities between trout and varanid lizards so far, it seems plausible that Na^+ accumulation is involved.

The second factor is SERCA activity, which could be operating maximally at higher frequencies in the absence of stimulation by catecholamines. Even without PKA dependent phosphorylation of phospholamban, high diastolic Ca^{2+} could increase SERCA pumping rate by activation of CaMKII (11, 34), but this pathway has yet to be investigated in ectotherms and the present data do not suggest a large role.

Thirdly, the reduced time at diastolic membrane potentials at higher frequencies would limit Ca^{2+} extrusion via forward-mode NCX. Indeed, when diastolic $[Ca^{2+}]_i$ is plotted against the

percent time at resting membrane potential, calculated as (1-[(APD_{90})/(period at each frequency)] x 100), the positive correlation is impressive (Fig. 5). However, more experimental evidence is required to confirm the mechanistic causes of Ca^{2+} accumulation.

Regardless of the mechanism by which it increases, our data suggests that elevated diastolic $[Ca^{2+}]_i$ plays a key role in the negative FFR. Contractility is directly related to the amplitude of the Ca^{2+} transient, 65% of which is transarcolemmal and 35% is SR in origin in this species at 20-22°C when paced at 0.2 Hz (21). Ca^{2+} release from both sites has been shown to be subject to some form of Ca^{2+}-dependent inactivation in mammals (9, 15, 16, 44) and could lead to the frequency-dependent reduction in $[Ca^{2+}]_i$ transient amplitude and rise slopes. A role for incomplete recovery from inactivation of the $I_{Ca\text{-}L}$ between beats at high frequencies seems unlikely as complete recovery is achieved in ~300 ms in this species (21). Further experimental work is required to test this directly.

Perspectives and Significance

There are always concerns when projecting findings from isolated myocytes to the working heart *in vivo.* However, the fact that we observed a negative FFR at the level of the isolated cardiomyocytes strongly suggests intrinsic cellular pathways may be responsible for the previously reported observations at the tissue level (18). Our experimental frequencies were chosen because they represent *in vivo* heart rates of varanid lizards near the temperature we studied them (20-22°C). At 25°C, varanid lizards have a resting heart rate of 0.4 Hz and a maximum of 0.85 Hz (10). Stroke volume at maximal heart rate is 60% higher than at rest which, combined with the heart rate changes, leads to an approximate tripling of cardiac output. Therefore the reduction in contractility observed in isolated cardiomyocytes and in muscle strips

(18) at high frequencies does not correlate with whole animal cardiac function. It is likely that under conditions when maximum heart rates are achieved, such as with exercise, some extrinsic factor plays a role in maintaining cardiac contractility. Under such conditions, there is likely to be significant β-adrenergic stimulation that could increase $I_{Ca\text{-}L}$ or SERCA activity or decrease the myofilament sensitivity to Ca^{2+} (22), which would probably increase resting length to promote more diastolic filling. Adrenaline increases force production in ventricular strips from varanids (18) and in ventricular trabeculae from trout (40). Its specific effects in isolated ventricular myocytes require further study. Unfortunately, any study of adrenaline is complicated by the lack of any *in vivo* measurements of plasma catecholamines from varanids.

Acknowledgments

We wish to thank Drs Fabien Brette and Tony Farrell for their helpful discussion during the preparation of this manuscript. Present address for D.E.W.: Department of Anesthesia, University of California, San Francisco

Grants

This research was supported by a BBSRC grant to H.A.S.

References

1. **Bers DM.** Ca influx and sarcoplasmic reticulum Ca release in cardiac muscle activation during postrest recovery. *Am J Physiol* 248: H366-381, 1985.

2. **Bers DM.** Calcium cycling and signaling in cardiac myocytes. *Annu Rev Physiol* 70: 23-49, 2008.

3. **Bers DM.** Cardiac excitation-contraction coupling. *Nature* 415: 198-205, 2002.

4. **Bers DM.** *Excitation-Contraction Coupling and Cardiac Contractile Force*. Boston: Kluwer, 2001.

5. **Birkedal R and Shiels HA.** High [Na+]i in cardiomyocytes from rainbow trout. *Am J Physiol Regul Integr Comp Physiol* 293: R861-866, 2007.

6. **Bossen EH and Sommer JR.** Comparative stereology of the lizard and frog myocardium. *Tissue Cell* 16: 173-178, 1984.

7. **Bowditch HP.** Uber die Eigenthümlichkeiten der Reizbarkeit, welche die Muskelfasem des Herzens zeigen. *Ber Sachs Ges Wiss* 23: 652-689, 1871.

8. **Boyett MR, Hart G, Levi AJ, and Roberts A.** Effects of repetitive activity on developed force and intracellular sodium in isolated sheep and dog Purkinje fibres. *J Physiol* 388: 295-322, 1987.

9. **Ching LL, Williams AJ, and Sitsapesan R.** Evidence for Ca^{2+} activation and inactivation sites on the luminal side of the cardiac ryanodine receptor complex. *Circ Res* 87: 201-206, 2000.

10. **Clark TD, Wang T, Butler PJ, and Frappell PB.** Factorial scopes of cardio-metabolic variables remain constant with changes in body temperature in the varanid lizard, Varanus rosenbergi. *Am J Physiol Regul Integr Comp Physiol* 288: R992-997, 2005.

11. **DeSantiago J, Maier LS, and Bers DM.** Frequency-dependent acceleration of relaxation in the heart depends on CaMKII, but not phospholamban. *J Mol Cell Cardiol* 34: 975-984, 2002.

12. **Driedzic W and Gesser H.** Ca2+ protection from the negative inotropic effect of contraction frequency on teleost hearts. *J Comp Physiol B* 156: 135-142, 1985.

13. **Driedzic WR and Gesser H.** Differences in Force-Frequency Relationships and Calcium Dependency Between Elasmobranch and Teleost Hearts. *J Exp Biol* 140: 227-241, 1988.

14. **Endoh M.** Force-frequency relationship in intact mammalian ventricular myocardium: physiological and pathophysiological relevance. *Eur J Pharmacol* 500: 73-86, 2004.

15. **Fabiato A.** Time and calcium dependence of activation and inactivation of calcium-induced release of calcium from the sarcoplasmic reticulum of a skinned canine cardiac Purkinje cell. *J Gen Physiol* 85: 247-289, 1985.

16. **Findlay I.** Physiological modulation of inactivation in L-type Ca2+ channels: one switch. *J Physiol* 554: 275-283, 2004.

17. **Frampton JE, Harrison SM, Boyett MR, and Orchard CH.** Ca2+ and Na+ in rat myocytes showing different force-frequency relationships. *Am J Physiol* 261: C739-750, 1991.

18. **Galli GL, Gesser H, Taylor EW, Shiels HA, and Wang T.** The role of the sarcoplasmic reticulum in the generation of high heart rates and blood pressures in reptiles. *J Exp Biol* 209: 1956-1963, 2006.

19. **Galli GL, Lipnick MS, and Block BA.** Effect of thermal acclimation on action potentials and sarcolemmal K+ channels from Pacific bluefin tuna cardiomyocytes. *Am J Physiol Regul Integr Comp Physiol* 297: R502-509, 2009.

20. **Galli GL, Taylor EW, and Shiels HA.** Calcium flux in turtle ventricular myocytes. *Am J Physiol Regul Integr Comp Physiol* 291: R1781-1789, 2006.

21. **Galli GL, Warren DE, and Shiels H.** Ca^{2+} Cycling in Cardiomyocytes from a High Performance Reptile, the Varanid Lizard, *Varanus exanthematicus*. *Am J Physiol-Reg Integr Comp Physiol In Press*, 2009.

22. **Gambassi G, Spurgeon HA, Lakatta EG, Blank PS, and Capogrossi MC.** Different effects of alpha- and beta-adrenergic stimulation on cytosolic pH and myofilament responsiveness to Ca2+ in cardiac myocytes. *Circ Res* 71: 870-882, 1992.

23. **Gillis TE, Marshall CR, Xue XH, Borgford TJ, and Tibbits GF.** Ca(2+) binding to cardiac troponin C: effects of temperature and pH on mammalian and salmonid isoforms. *Am J Physiol Regul Integr Comp Physiol* 279: R1707-1715, 2000.

24. **Gleeson TT, Mitchell GS, and Bennett AF.** Cardiovascular responses to graded activity in the lizards Varanus and Iguana. *Am J Physiol* 239: R174-179, 1980.

25. **Grynkiewicz G, Poenie M, and Tsien RY.** A new generation of Ca2+ indicators with greatly improved fluorescence properties. *J Biol Chem* 260: 3440-3450, 1985.

26. **Harwood CL, Howarth FC, Altringham JD, and White E.** Rate-dependent changes in cell shortening, intracellular Ca(2+) levels and membrane potential in single, isolated rainbow trout (Oncorhynchus mykiss) ventricular myocytes. *J Exp Biol* 203: 493-504, 2000.

27. **Haverinen J and Vornanen M.** Responses of Action Potential and K(+) Currents to Temperature Acclimation in Fish Hearts: Phylogeny or Thermal Preferences? *Physiol Biochem Zool*, 2009.

28. **Hove-Madsen L.** The influence of temperature on ryanodine sensitivity and the force-frequency relationship in the myocardium of rainbow trout. *J Exp Biol* 167: 47-60, 1992.

29. **Hussain M, Drago GA, Colyer J, and Orchard CH.** Rate-dependent abbreviation of Ca2+ transient in rat heart is independent of phospholamban phosphorylation. *Am J Physiol* 273: H695-706, 1997.

30. **Kondo N and Shibata S.** Calcium source for excitation-contraction coupling in myocardium of nonhibernating and hibernating chipmunks. *Science* 225: 641-643, 1984.

31. **Larsson D, Larsson B, Lundgren T, and Sundell K.** The effect of pH and temperature on the dissociation constant for fura-2 and their effects on [Ca(2+)](i) in enterocytes from a poikilothermic animal, Atlantic cod (Gadus morhua). *Anal Biochem* 273: 60-65, 1999.

32. **Li GR, Yang B, Feng J, Bosch RF, Carrier M, and Nattel S.** Transmembrane ICa contributes to rate-dependent changes of action potentials in human ventricular myocytes. *Am J Physiol* 276: H98-H106, 1999.

33. **Li L, Chu G, Kranias EG, and Bers DM.** Cardiac myocyte calcium transport in phospholamban knockout mouse: relaxation and endogenous CaMKII effects. *Am J Physiol* 274: H1335-1347, 1998.

34. **Maier LS and Bers DM.** Role of Ca2+/calmodulin-dependent protein kinase (CaMK) in excitation-contraction coupling in the heart. *Cardiovasc Res* 73: 631-640, 2007.

35. **Patel SP and Campbell DL.** Transient outward potassium current, 'Ito', phenotypes in the mammalian left ventricle: underlying molecular, cellular and biophysical mechanisms. *J Physiol* 569: 7-39, 2005.

36. **Ravens U and Wettwer E.** Electrophysiological aspects of changes in heart rate. *Basic Res Cardiol* 93 Suppl 1: 60-65, 1998.

37. **Rumberger E and Reichel H.** The force-frequency relationship: a comparative study between warm- and cold-blooded animals. *Pflugers Arch* 332: 206-217, 1972.

38. **Sah R, Ramirez RJ, Oudit GY, Gidrewicz D, Trivieri MG, Zobel C, and Backx PH.** Regulation of cardiac excitation-contraction coupling by action potential repolarization: role of the transient outward potassium current (I(to)). *J Physiol* 546: 5-18, 2003.

39. **Shattock MJ and Bers DM.** Inotropic response to hypothermia and the temperature-dependence of ryanodine action in isolated rabbit and rat ventricular muscle: implications for excitation-contraction coupling. *Circ Res* 61: 761-771, 1987.

40. **Shiels H and Farrell A.** The effect of temperature and adrenaline on the relative importance of the sarcoplasmic reticulum in contributing Ca2+ to force development in isolated ventricular trabeculae from rainbow trout. *J Exp Biol* 200: 1607-1621, 1997.

41. **Shiels HA and Farrell AP.** The effect of temperature and adrenaline on the relative importance of the sarcoplasmic reticulum in contributing Ca2+ to force development in isolated ventricular trabeculae from rainbow trout. *J Exp Biol* 200: 1607-1621, 1997.

42. **Shiels HA, Vornanen M, and Farrell AP.** Effects of temperature on intracellular Ca2+ in trout atrial myocytes. *J Exp Biol* 205: 3641-3650, 2002.

43. **Shiels HA, Vornanen M, and Farrell AP.** The force-frequency relationship in fish hearts--a review. *Comp Biochem Physiol A Mol Integr Physiol* 132: 811-826, 2002.

44. **Sitsapesan R and Williams AJ.** Do inactivation mechanisms rather than adaptation hold the key to understanding ryanodine receptor channel gating? *J Gen Physiol* 116: 867-872, 2000.

45. **Stecyk JA, Paajanen V, Farrell AP, and Vornanen M.** Effect of temperature and prolonged anoxia exposure on electrophysiological properties of the turtle (Trachemys scripta) heart. *Am J Physiol Regul Integr Comp Physiol* 293: R421-437, 2007.

46. **Tijskens P, Meissner G, and Franzini-Armstrong C.** Location of ryanodine and dihydropyridine receptors in frog myocardium. *Biophys J* 84: 1079-1092, 2003.

47. **Valverde CA, Mundina-Weilenmann C, Said M, Ferrero P, Vittone L, Salas M, Palomeque J, Petroff MV, and Mattiazzi A.** Frequency-dependent acceleration of relaxation in mammalian heart: a property not relying on phospholamban and SERCA2a phosphorylation. *J Physiol* 562: 801-813, 2005.

48. **Varro A, Lathrop DA, Hester SB, Nanasi PP, and Papp JG.** Ionic currents and action potentials in rabbit, rat, and guinea pig ventricular myocytes. *Basic Res Cardiol* 88: 93-102, 1993.

49. **Vornanen M, Ryokkynen A, and Nurmi A.** Temperature-dependent expression of sarcolemmal K(+) currents in rainbow trout atrial and ventricular myocytes. *Am J Physiol Regul Integr Comp Physiol* 282: R1191-1199, 2002.

50. **Walden AP, Dibb KM, and Trafford AW.** Differences in intracellular calcium homeostasis between atrial and ventricular myocytes. *J Mol Cell Cardiol* 46: 463-473, 2009.

51. **Wang DY, Chae SW, Gong QY, and Lee CO.** Role of aiNa in positive force-frequency staircase in guinea pig papillary muscle. *Am J Physiol* 255: C798-807, 1988.

52. **Wang T, Carrier DR, and Hicks JW.** Ventilation and gas exchange in lizards during treadmill exercise. *J Exp Biol* 200: 2629-2639, 1997.

53. **Woodworth RS.** Maximal Contraction, "Staircase" Contraction, Refractory Period, and Compensatory Pause, of the Heart. *Am J Phyiol* 8: 213-249, 1902.

54. **Yue DT.** Relationships between intracellular free calcium and force with changes of interval. In: *The Interval-Force Relationship of the Heart: Bowditch revisited*, edited by Noble MIM and Seed WA. Cambridge: Cambridge University Press, 1992, p. 95-110.

Figure 1. The effect of frequency on sarcomere shortening in varanid lizard ventricular myocytes. (A) Representative traces from a varanid lizard ventricular myocyte tested at 0.2, 0.3, 0.5, 0.8 and 1.0 Hz. (B) Sarcomere shortening velocity, (C) diastolic sarcomere (sarc.) length as a percentage of that at 0.2 Hz, (D) sarcomere shortening as a percentage of diastolic length, and (E) the time required to recover to 50% of peak shortening. ○ represents the measurement upon return to 0.2 Hz. All values are means ± SEM, $n = 8$. Differing letters indicate statistical differences ($P<0.05$).

Figure 2. The effect of frequency on intracellular Ca^{2+} in varanid lizard ventricular myocytes. (A) Representative traces from a varanid lizard ventricular myocyte tested at 0.2, 0.3, 0.5, 0.8 and 1.0 Hz. (B) $[Ca^{2+}]_i$ rise slope, (C) diastolic $[Ca^{2+}]_i$, (D) $[Ca^{2+}]_i$ transient amplitude, and (E) τ, the time constant of the $[Ca^{2+}]_i$ transient decay. ○ represents the measurement upon return to 0.2 Hz. All values are means ± SEM, $n = 7$. Differing letters indicate statistical differences ($P<0.05$).

Figure 3. The effect of frequency on action potential (AP) characteristics in varanid lizard ventricular myocytes. (A) Representative traces from a varanid lizard ventricular myocyte tested at 0.3, 0.5, 0.8 and 1.0 Hz. (B) The rate of rise of the AP, (C) resting membrane potential, (D) peak membrane potential reached during depolarization, and (E) AP duration at 50% (APD_{50}) and 90% (APD_{50}) of hyperpolarization. ○ and Δ represent measurements upon return to to 0.3 Hz. All values are means ± SEM, $n = 7$. Differing letters indicate statistical differences$P<0.05$).

Figure 4. The effect of frequency on the current-voltage relationship of the background inward rectifier current (I_{K1}) in varanid lizard ventricular myocytes. (A) Voltage protocol used to isolate I_{K1}. I_{K1} was measured by applying repolarizing voltage ramps (1 s) from 30 mV to -120 at 5 s intervals in the absence and presence of $BaCl_2$ (500 μM). I_{K1} was then calculated as the Ba^{2+}-sensitive current. (B) A representative current trace elicited from the voltage protocol in (A). (C) Mean ± SEM (n = 7) for I_{K1} current-voltage relationship measured at 0.3Hz.

Figure 5. Diastolic $[Ca^{2+}]_i$ versus percent time at resting membrane potential (Vm), which is calculated as (1-[(APD_{90})/(period at each frequency)] x 100).

Table 1. *The effects of frequency on the shortening of varanid lizard ventricular myocytes.*

	0.2 Hz	0.3 Hz	0.5 Hz	0.8 Hz	1.0 Hz	0.2 Hz
Cell Shortening (% Change from rest)	7.74 ± 1.60^{a}	$7.04 \pm 1.35^{a,b}$	$5.50 \pm 1.41^{b,c}$	5.30 ± 1.11^{b}	4.31 ± 0.87^{c}	7.4 ± 1.30^{a}
Rate of Shortening (nm ms^{-1})*	18.3 ± 2.3^{a}	22.0 ± 4.8^{a}	22.9 ± 7.9^{a}	34.3 ± 16.5^{a}	17.4 ± 4.1^{a}	18.3 ± 4.5^{a}
Time to Peak Shortening (ms)*	660 ± 78^{a}	525 ± 30^{b}	439 ± 48^{c}	400 ± 60^{c}	410 ± 29^{c}	727 ± 81^{a}
Time to 50% relaxation (ms)	256 ± 24^{a}	286 ± 28^{a}	220 ± 24^{a}	146 ± 15^{b}	135 ± 23^{b}	230 ± 27^{a}

Values are means ± SEM, $n = 8$ per group from 4 animals
Differing letters indicate statistical differences (one-factor RM ANOVA; SNK post-hoc; $P<0.05$)
* indicates RM ANOVA on ranks.

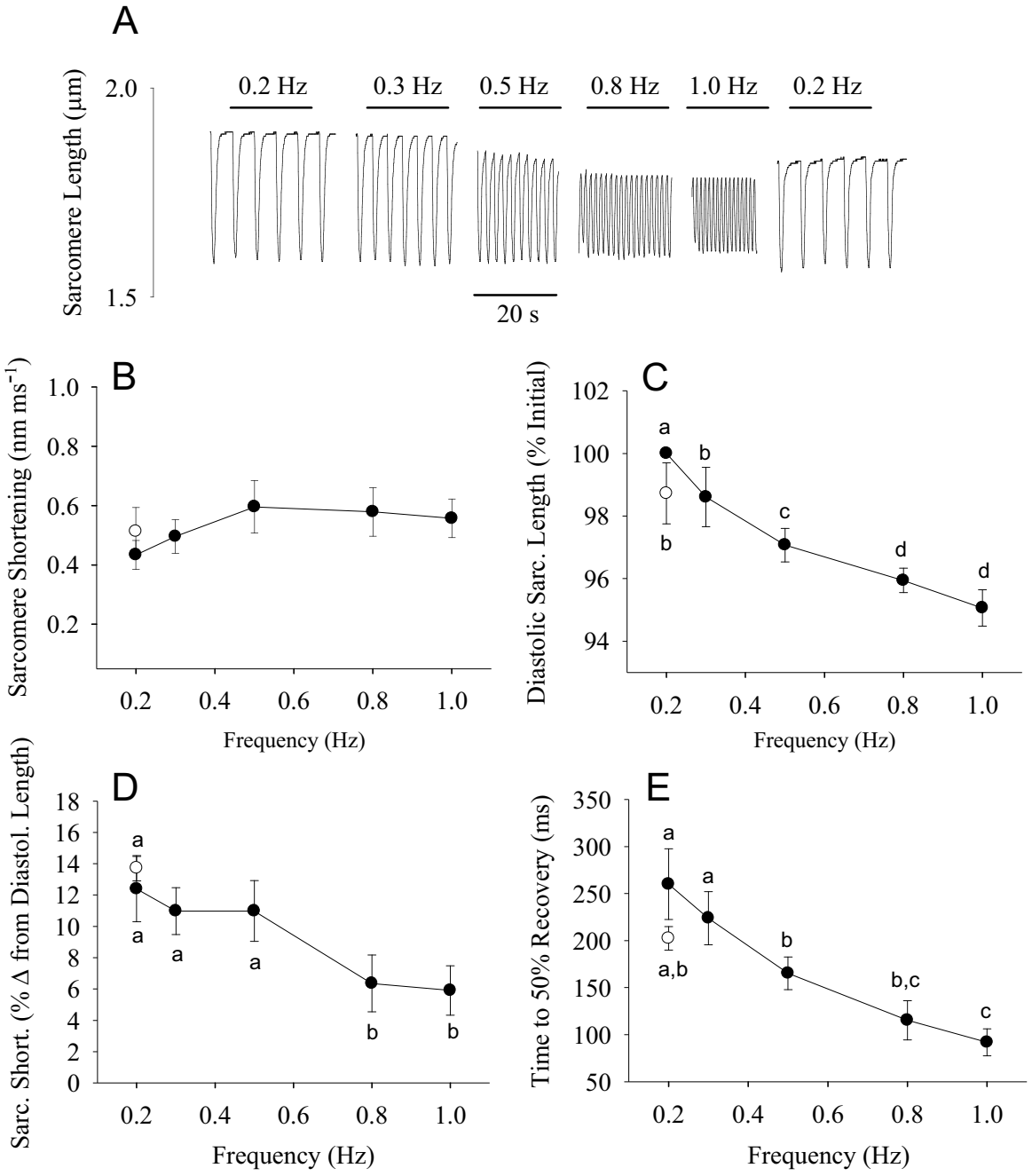
A
Sarcomere Length (µm)
2.0
1.5
0.2 Hz
0.3 Hz
0.5 Hz
0.8 Hz
1.0 Hz
0.2 Hz
20 s
B
Sarcomere Shortening (nm ms-1)
Frequency (Hz)
C
Diastolic Sarc. Length (% Initial)
Frequency (Hz)
D
Sarc. Short. (% Δ from Diastol. Length)
Frequency (Hz)
E
Time to 50% Recovery (ms)
Frequency (Hz)

Figure 1

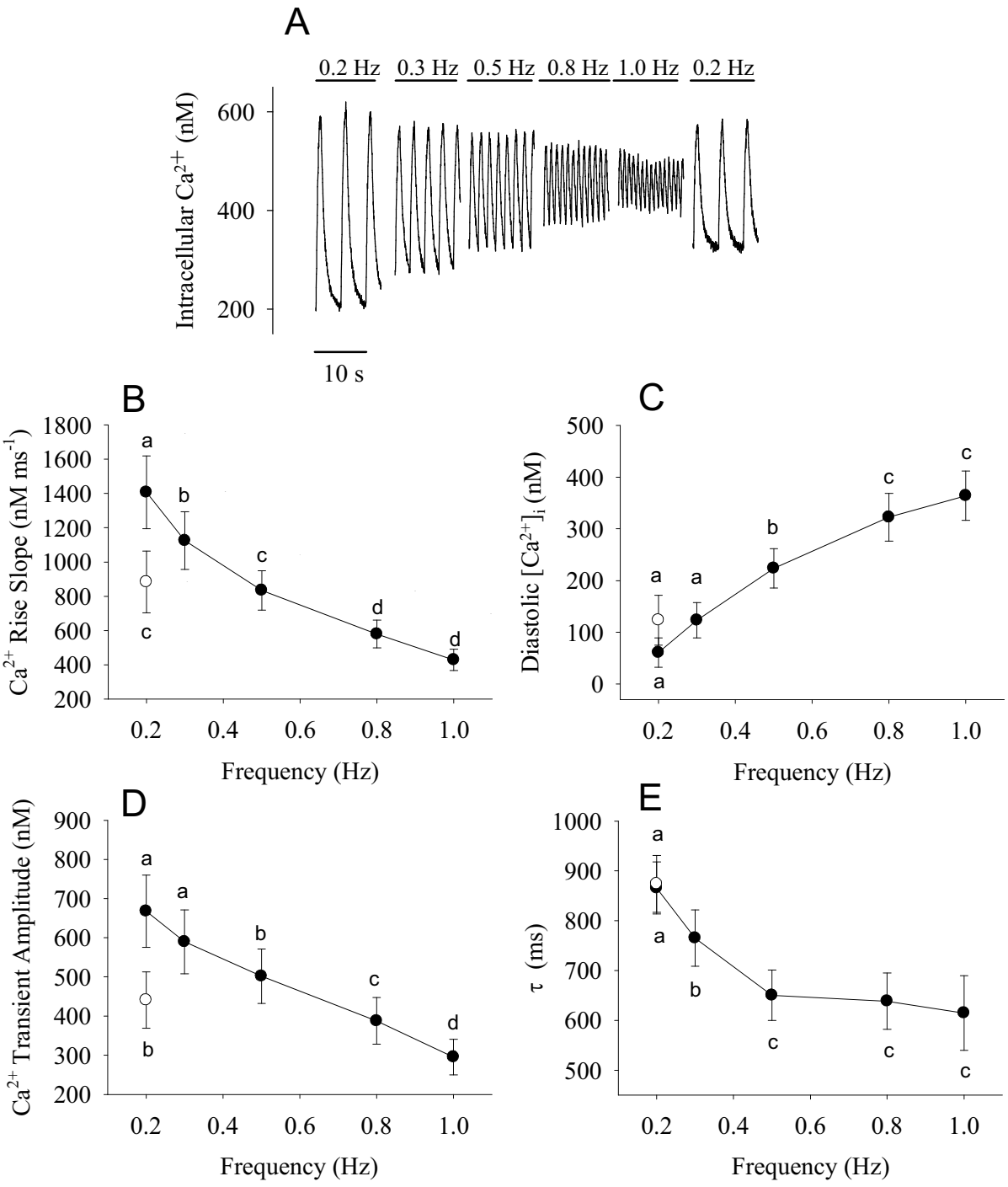
A
0.2 Hz
0.3 Hz
0.5 Hz
0.8 Hz
1.0 Hz
0.2 Hz
Intracellular Ca2+ (nM)
600
400
200
10 s
B
Ca2+ Rise Slope (nM ms-1)
1800
1600
1400
1200
1000
800
600
400
200
a
b
c
d
d
c
0.2
0.4
0.6
0.8
1.0
Frequency (Hz)
C
Diastolic [Ca2+]i (nM)
500
400
300
200
100
0
a
a
b
c
c
a
0.2
0.4
0.6
0.8
1.0
Frequency (Hz)
D
Ca2+ Transient Amplitude (nM)
900
800
700
600
500
400
300
200
a
a
b
c
d
b
0.2
0.4
0.6
0.8
1.0
Frequency (Hz)
E
τ (ms)
1000
900
800
700
600
500
a
a
b
c
c
c
0.2
0.4
0.6
0.8
1.0
Frequency (Hz)

Figure 2

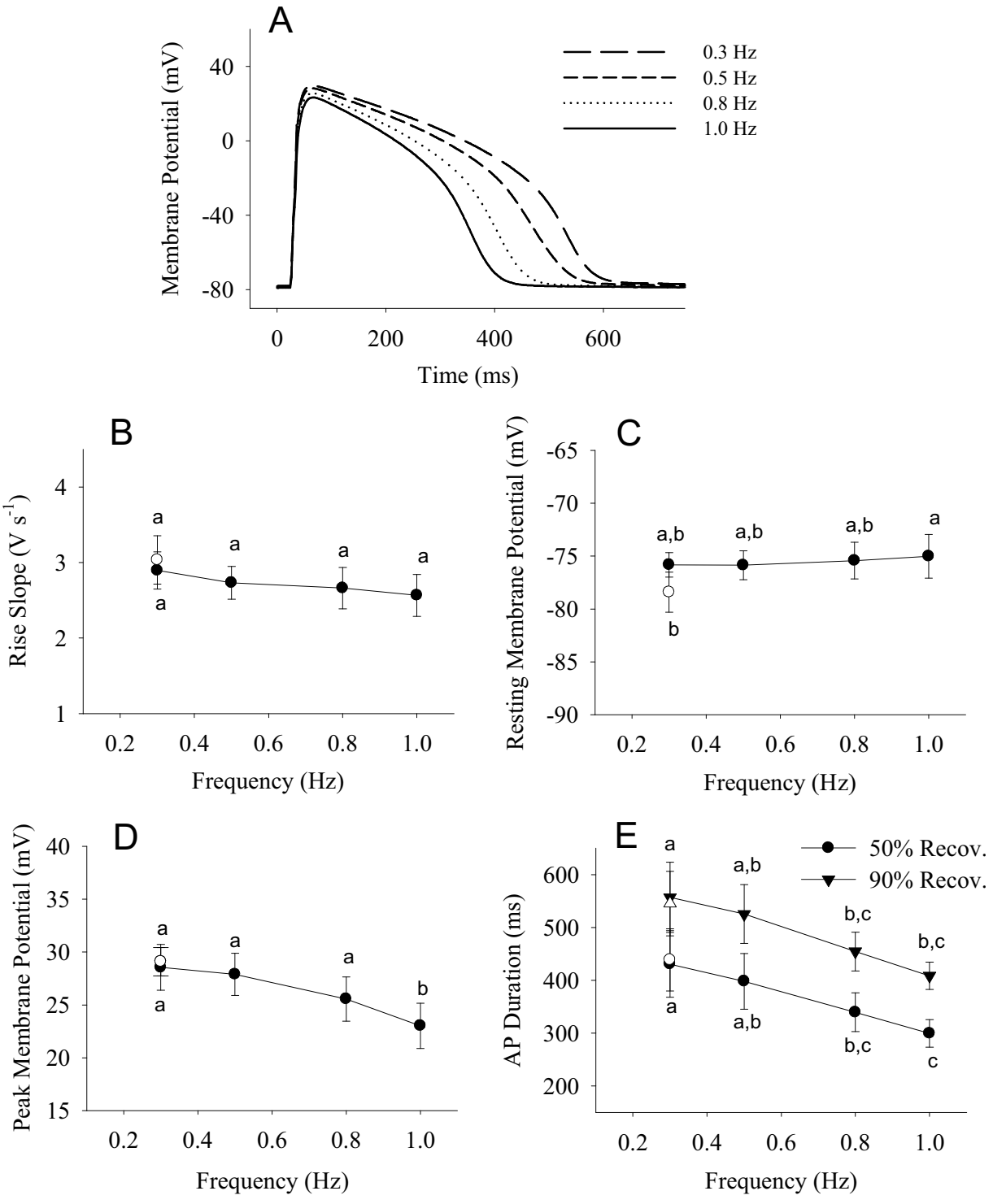
A
Membrane Potential (mV)
40
0
-40
-80
0
200
400
600
Time (ms)
0.3 Hz
0.5 Hz
0.8 Hz
1.0 Hz
B
Rise Slope (V s-1)
4
3
2
1
a
a
a
a
a
0.2
0.4
0.6
0.8
1.0
Frequency (Hz)
C
Resting Membrane Potential (mV)
-65
-70
-75
-80
-85
-90
a,b
a,b
a,b
a
b
0.2
0.4
0.6
0.8
1.0
Frequency (Hz)
D
Peak Membrane Potential (mV)
40
35
30
25
20
15
a
a
a
a
b
0.2
0.4
0.6
0.8
1.0
Frequency (Hz)
E
AP Duration (ms)
600
500
400
300
200
50% Recov.
90% Recov.
a
a,b
b,c
b,c
a
a,b
b,c
c
0.2
0.4
0.6
0.8
1.0
Frequency (Hz)

Figure 3

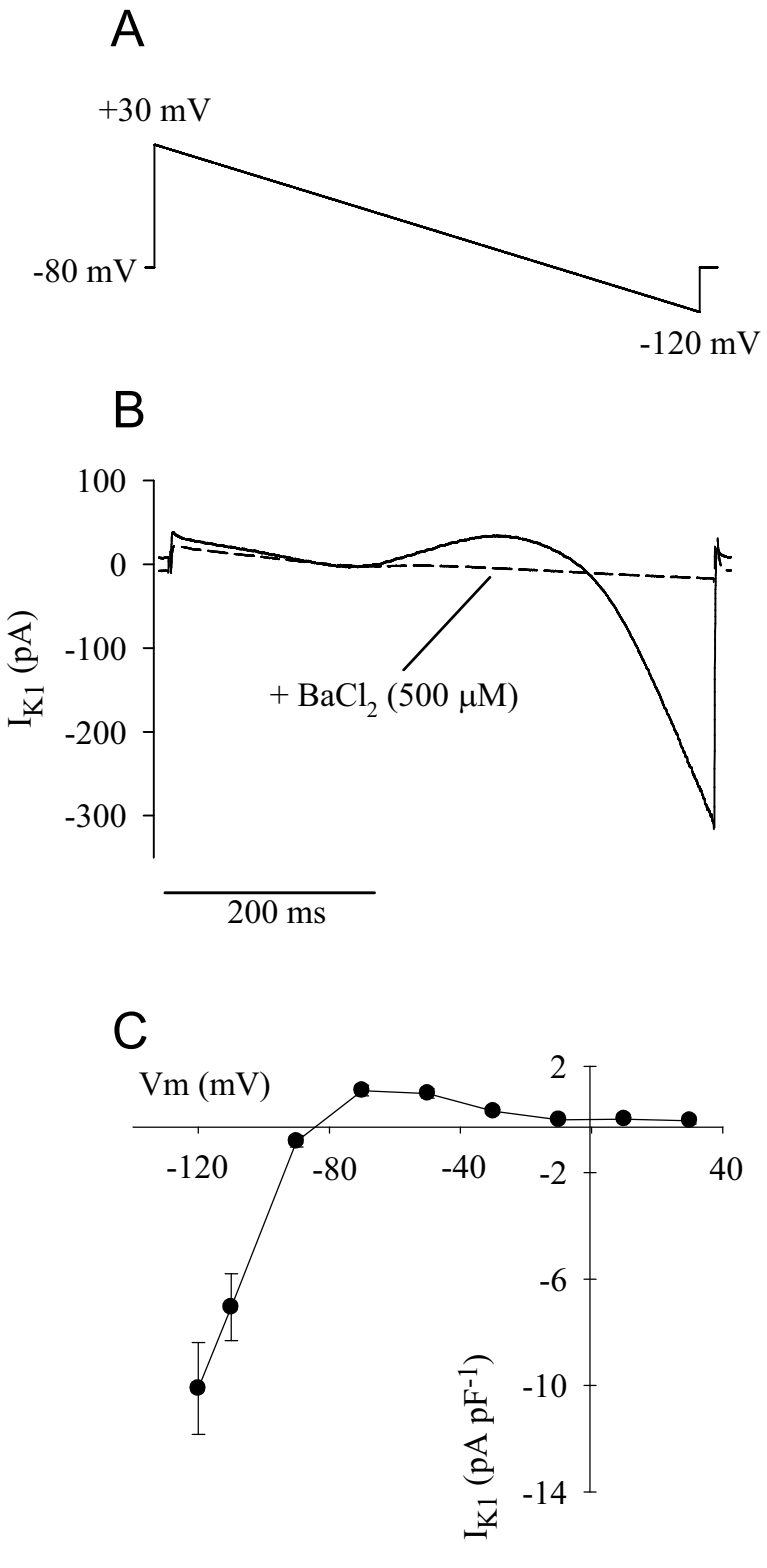
A
+30 mV
-80 mV
-120 mV
B
100
0
-100
-200
-300
I_{K1} (pA)
+ $BaCl_2$ (500 μM)
200 ms
C
Vm (mV)
-120
-80
-40
2
-2
40
-6
-10
-14
I_{K1} (pA pF^{-1})

Figure 4

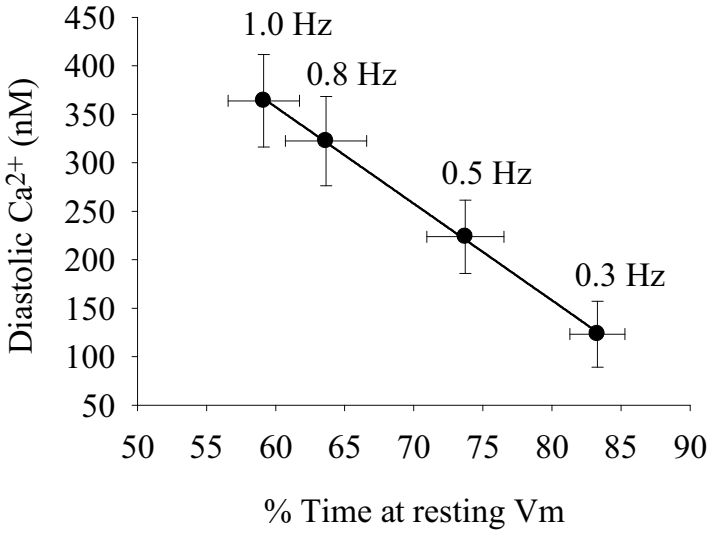
1.0 Hz
0.8 Hz
0.5 Hz
0.3 Hz
Diastolic Ca2+ (nM)
450
400
350
300
250
200
150
100
50
50
55
60
65
70
75
80
85
90
% Time at resting Vm

Figure 5